First observation of candidate chiral doublet bands in $Z = 37$ Rb isotopes

X. C. Han (韩星池), S. Y. Wang (王守宇),* B. Qi (亓斌), C. Liu (刘晨), S. Wang (王硕), D. P. Sun (孙大鹏), Z. Q. Li (李志泉), H. Jia (贾慧), R. J. Guo (郭睿巨), X. Xiao (肖骁), L. Mu (穆琳), X. Lu (陆晓), Q. Wang (王强), W. Z. Xu (许文政), and H. W. Li (李弘伟)
Shandong Provincial Key Laboratory of Optical Astronomy and Solar-Terrestrial Environment, Institute of Space Sciences, Shandong University, Weihai 264209, People's Republic of China

X. G. Wu (吴晓光), Y. Zheng (郑云), C. B. Li (李聪博), T. X. Li (李天晓), and Z. Y. Huang (黄智勇)
China Institute of Atomic Energy, Beijing 102413, People's Republic of China

H. Y. Wu (吴鸿毅) and D. W. Luo (罗迪雯)
State Key Laboratory of Nuclear Physics and Technology, School of Physics, Peking University, Beijing 100871, People's Republic of China

(Received 2 December 2020; revised 17 May 2021; accepted 15 July 2021; published 30 July 2021)

High-spin states in ^{84}Rb have been studied using the ^{76}Ge(^{11}B, $3n$) reaction at a beam energy of 36 MeV. A pair of nearly degenerate positive-parity doublet bands have been extended and interpreted as candidate chiral doublet bands based on their experimental properties. This interpretation is supported by the triaxial relativistic mean-field theory and the triaxial particle-rotor model calculations. The systematic comparison of the candidate chiral bands in the $A \approx 80$ mass region are also discussed. This work is the first observation of candidate chiral doublet bands in $Z = 37$ Rb isotopes and extends the boundaries of the chiral nuclei in the $A \approx 80$ mass region.

DOI: 10.1103/PhysRevC.104.014327

I. INTRODUCTION

In 1997, Frauendorf and Meng [1] pointed out that rotating triaxial nucleus may exhibit chiral geometry. The ideal chiral geometry in nuclei entails the angular momentum vectors of the valence proton, valance neutron, and core are mutually perpendicular to each other, thereby forming either a left- or a right-handed system. The experimental signal of the chiral symmetry breaking in nuclei is the observation of chiral doublet bands, which are a pair of nearly degenerate $\Delta I = 1$ bands with the same parity. So far, candidate chiral doublet bands have been reported experimentally in the $A \approx 80$, 100, 130, and 190 mass regions of the nuclear chart; see recent reviews [2–10] and references therein.

The $A \approx 80$ mass region is a recently identified chiral region where only three cases of candidate chiral nuclei have been reported in Br isotopes [11–13]. In 2011, a pair of candidate chiral doublet bands was observed in ^{80}Br, which provided the first evidence for chirality in the $A \approx 80$ mass region, and gave a new chiral configuration $\pi g_{9/2} \otimes \nu g_{9/2}$ [11]. Subsequently, the first evidence for the multiple chiral doublet bands with octupole correlations was found in ^{78}Br [12]. This observation indicated that nuclear chirality can be robust against the octupole correlations, and a simultaneous breaking of chiral and space-reflection symmetries may exist in a single nucleus. Very recently, a pair of candidate chiral doublet bands was observed in ^{82}Br [13], which extended the border of the chiral nuclei in the $A \approx 80$ mass region to $N = 47$. Reference [13] suggested that the chiral geometry in ^{82}Br is more stable than those in ^{78}Br and ^{80}Br based on the calculated coupling pattern of the angular momentum. It is naturally interesting to find more chiral candidates and explore the boundaries of the chiral nuclei in the $A \approx 80$ mass region. The present work identifies candidate chiral doublet bands in ^{84}Rb ($Z = 37$), and provides the first evidence for candidate chiral nuclei in the A ≈ 80 mass region beyond the Br isotopes.

II. EXPERIMENTAL DETAILS

Excited states of ^{84}Rb were populated via the reaction ^{76}Ge(^{11}B, $3n$) at a beam energy of 36 MeV using the HI-13 tandem accelerator at the China Institute of Atomic Energy (CIAE). The target consisted of 1 mg/cm^2 ^{76}Ge evaporated on a 10 mg/cm^2 gold backing. The emitted γ rays were detected by an array of six Compton-suppressed high-purity germanium (HPGe) detectors and one clover detector. The detectors were placed at 90° (two HPGe and the clover), 42° (two HPGe), 140° (one HPGe), and 150° (one HPGe) with respect to the beam axis. Approximately 3.8×10^7 γ-γ coincidence events were recorded in prompt coincidence (<150 ns) with a general-purpose digital data acquisition system (GDDAQ) [14] based on Pixie-16 modules from XIA LLC [15].

In the offline analysis, energy and efficiency calibrations of these detectors were achieved using standard ^{133}Ba and ^{152}Eu radioactive sources placed at the target position.

*sywang@sdu.edu.cn

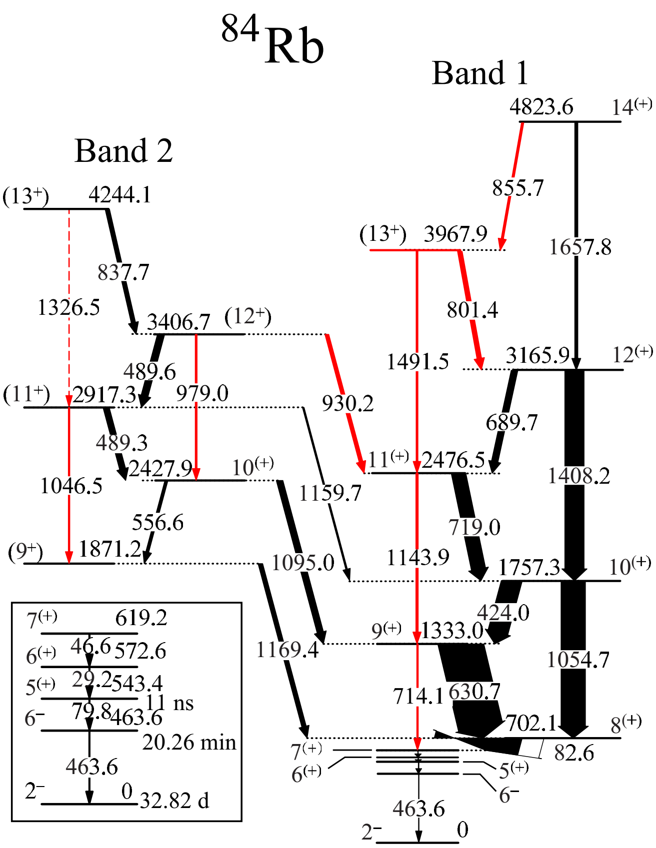

FIG. 1. Partial level scheme of ^{84}Rb deduced from the present work. The newly observed transitions and level are in red. All the observed transitions in the present work eventually feed into $7^{(+)}$ state at 619.2 keV. The experimental information below the $7^{(+)}$ state was taken from Refs. [22,23], and is given in the inset with an expanded view.

The gain-matched data were sorted into one symmetric and two asymmetric matrices used for γ-ray coincidence and angular distributions from the oriented states (ADO) [16] analyses, respectively. The typical ADO ratios were extracted from the strong transitions of known multipolarities in ^{83}Rb [17]. In the present geometry, the typical ADO ratio $\approx$1.4 is expected for the stretched quadrupole or $\Delta I = 0$ dipole transitions and ≈ 0.8 for the pure stretched dipole ones.

III. RESULTS AND DISCUSSION

Prior to the present work, High-spin states of ^{84}Rb have been studied by two groups [18–21]. Based on the present γ-γ coincidence relationships, energy and intensity balances, we constructed the level structures of ^{84}Rb. The updated partial level scheme of ^{84}Rb is given in Fig. 1, in which the two positive-parity rotational bands are labeled as bands 1 and 2. Spectra showing the newly identified transitions in ^{84}Rb are given in Fig. 2. For the placements of γ rays in the positive-parity bands, there exist some differences between Refs. [20,21]. For example, the 719.0 keV γ transition decayed into the $10^{(+)}$ state at 1757.3 keV was rather strong in Ref. [20] while it was very weak (shown as a dashed line) in Ref. [21]. In order to clarify the difference, the sample spectrum gated on 424.0 keV was given in Fig. 3. As shown in Fig. 3, the strong 719.0 keV transition and the existence of the 689.7 and 1159.7 keV transitions supported the present placements of γ rays in Fig. 1, which are consistent with those in Ref. [20].

In the present work, the spin-parity assignments are deduced from the measured ADO ratios. It should be noted that there exist a contradiction in the spin assignment for the 2427.9 keV state between Refs. [20] and [21]. Reference [20] assigned $10^{(+)}$ for the 2427.9 keV state, while the same state was assigned as $11^{(+)}$ in Ref. [21]. This contradiction is caused by the different multipolarity for the 1095.0 keV transition linking the 2427.9 keV state to the $9^{(+)}$ state at 1333.0 keV. Based on the present ADO measurement, the ADO ratio of the 1095.0 keV transition is 1.08(0.09), which indicates an $M1/E2$ character. Therefore, the 2427.9 keV state was proposed as $I^{\pi} = 10^{(+)}$ in the present work. A new level at 3966.6 keV identified in this work connected the $12^{(+)}$ and $11^{(+)}$ states in band 1 through the 801.4 and 1491.5 keV transitions, respectively. The ADO ratio of the 801.4 keV transition is 0.75(0.20), which indicates an $M1/E2$ or $E1$ character. We adopted the $M1/E2$ character for the 801.4 keV transition due to the empirical rotational band structure of band 1. Therefore, we assigned (13^{+}) for the newly observed level. Based on the same reasons, the spin-parity of the highest observed state in band 2 was tentatively suggested as (13^{+}). The excitation energies, spin-parity assignments for the initial and final states, the transition energies, relative intensities, and ADO ratios of the γ rays in ^{84}Rb are listed in Table I.

In 1991, the yrast states from $5^{(+)}$ to $10^{(+)}$ in ^{84}Rb have been assigned the $\pi g_{9/2} \otimes \nu g_{9/2}$ configuration based on the systematic comparison of the energy spacings with the neighboring odd-odd Br isotopes [23]. Thanks to the experimental progress in high-spin states of the odd-odd Rb isotopes [20,24–26], it allowed us to perform a systematic comparison of the energy spacings for the ^{76,78,80,82,84}Rb isotopes. Figure 4 presents the systematics of the excitation energies for the positive-parity yrast states in ^{76,78,80,82,84}Rb. As shown in Fig. 4, the energy levels of yrast bands in ^{76,78,80,82,84}Rb have a smooth systematic trend. It indicates that the yrast band in ^{84}Rb have the same physical origin as those in ^{76,78,80,82}Rb isotopes. The yrast bands in ^{76,78,80,82}Rb have been already assigned the $\pi g_{9/2} \otimes \nu g_{9/2}$ configuration [20,24–26]. Therefore, we suggested the $\pi g_{9/2} \otimes \nu g_{9/2}$ configuration to the positive-parity yrast band in ^{84}Rb. As shown in Fig. 1, band 2 feeds into band 1 through several $M1/E2$ linking transitions, which implies that band 2 is built on the same $\pi g_{9/2} \otimes \nu g_{9/2}$ configuration as band 1 [27–29].

The excitation energies $E(I)$, energy staggering parameters $S(I) = [E(I) - E(I-1)]/2I$, and $B(M1)/B(E2)$ ratios for the positive-parity doublet bands in ^{84}Rb as a function of spin are provided in Fig. 5. As shown in Fig. 5, bands 1 and 2 have a small energy difference and a relatively smooth variation of $S(I)$ values. The $B(M1)/B(E2)$ ratios for the two bands are close to each other and show odd-even staggering with the same phase as a function of spin. These experimental properties are consistent with the fingerprints of chiral doublet bands [4,30–32]. Therefore, the positive-parity doublet

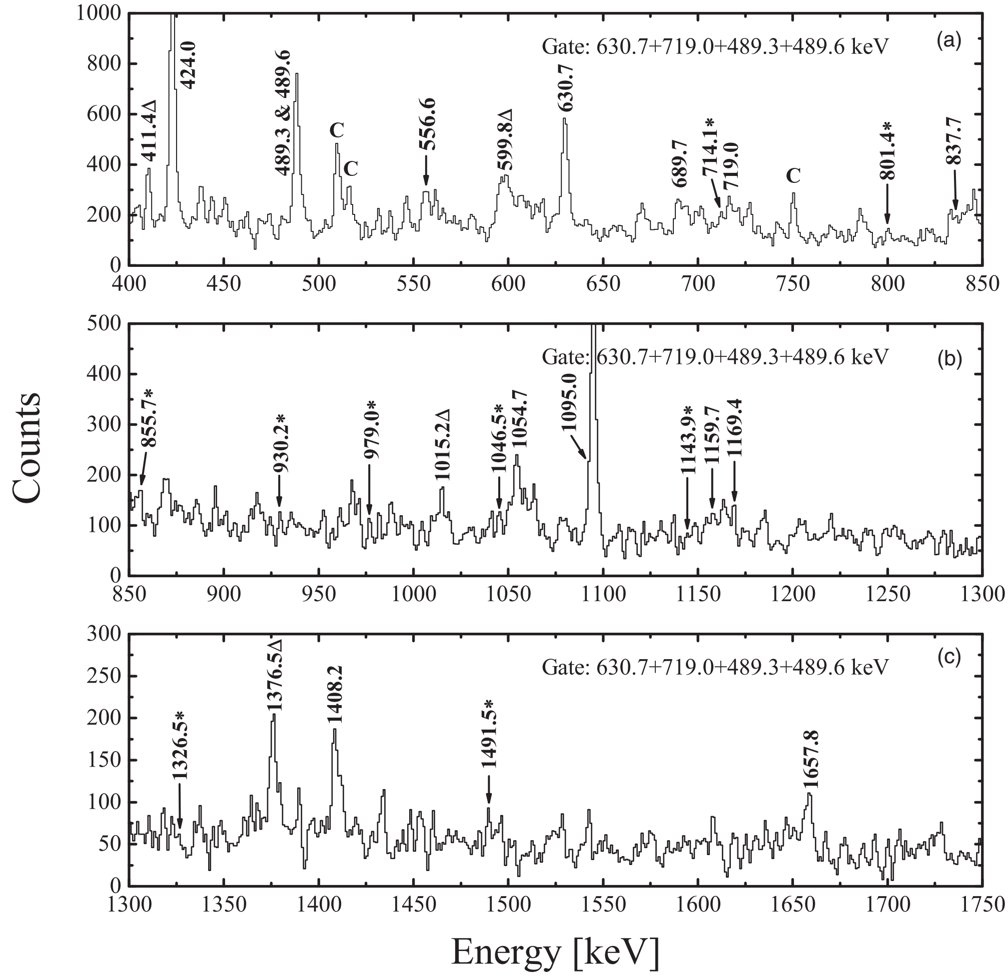

FIG. 2. The γ-ray coincidence spectra gated on the 630.7 + 719.0 + 489.3 + 489.6 keV transitions in ^{84}Rb. Peaks marked with asterisks are new in the present work. The transitions marked with triangles belong to ^{84}Rb and are not included in Fig. 1. Contaminants are denoted with C.

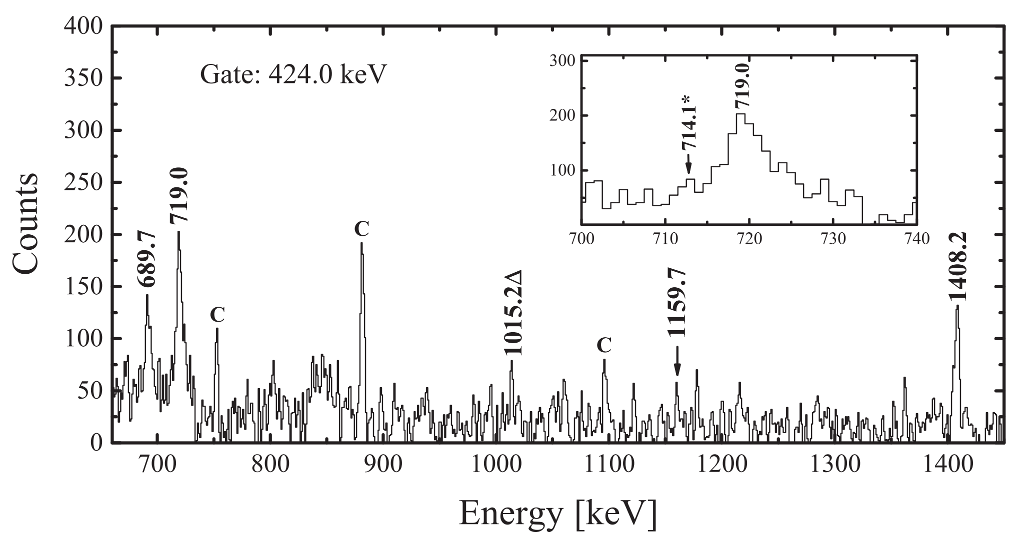

FIG. 3. The γ-ray coincidence spectrum gated on the 424.0 keV transition in ^{84}Rb. The inset is a section of the same spectrum expanded. The transitions marked with triangles belong to ^{84}Rb and are not included in Fig. 1. Contaminants are denoted with C.

TABLE I. The excitation energies and the spin-parity assignments for the initial and final states, the transition energies, relative intensities, and the measured ADO ratios of the γ rays in ^{84}Rb above the $J^{\pi} = 7^{(+)}$ state at 619.2 keV. The uncertainties in the energies of γ rays are 0.3 keV for intense ($I_{\gamma} > 10$) transitions and 0.7 keV for weak ($I_{\gamma} < 10$) transitions.

E_{γ} (keV)	E_i (keV)	E_f (keV)	$I_i^{\pi} \to I_f^{\pi}$	I_{γ}	ADO ratio
82.6	702.1	619.2	$8^{(+)} \to 7^{(+)}$	189.8(11.6)	0.74(0.09)
424.0	1757.3	1333.0	$10^{(+)} \to 9^{(+)}$	45.3(5.9)	0.89(0.06)
489.3	2917.3	2427.9	$(11^{+}) \to 10^{(+)}$	13.6(4.9)	0.93(0.08)
489.6	3406.7	2917.3	$(12^{+}) \to (11^{+})$	15.5(5.2)	0.93(0.08)
556.6	2427.9	1871.2	$10^{(+)} \to (9^{+})$	6.6(1.0)	
630.7	1333.0	702.1	$9^{(+)} \to 8^{(+)}$	100(1.7)	0.81(0.11)
689.7	3165.9	2476.5	$12^{(+)} \to 11^{(+)}$	14.5(4.1)	0.79(0.11)
714.1	1333.0	619.2	$9^{(+)} \to 7^{(+)}$	3.3(1.7)	
719.0	2476.5	1757.3	$11^{(+)} \to 10^{(+)}$	32.0(0.9)	0.98(0.13)
801.4	3967.9	3165.9	$(13^{+}) \to 12^{(+)}$	10.4(3.7)	0.75(0.20)
837.7	4244.1	3406.7	$(13^{+}) \to (12^{+})$	9.6(2.7)	0.79(0.28)
855.7	4823.6	3967.9	$14^{(+)} \to (13^{+})$	5.1(3.3)	
930.2	3406.7	2476.5	$(12^{+}) \to 11^{(+)}$	8.4(4.4)	
979.0	3406.7	2427.9	$(12^{+}) \to 10^{(+)}$	4.1(2.1)	
1046.5	2917.3	1871.2	$(11^{+}) \to (9^{+})$	3.3(1.2)	
1054.7	1757.3	702.1	$10^{(+)} \to 8^{(+)}$	54.4(4.7)	1.38(0.20)
1095.0	2427.9	1333.0	$10^{(+)} \to 9^{(+)}$	14.3(2.6)	1.08(0.09)
1143.9	2476.5	1333.0	$11^{(+)} \to 9^{(+)}$	5.2(1.5)	
1159.7	2917.3	1757.3	$(11^{+}) \to 10^{(+)}$	3.6(1.2)	
1169.4	1871.2	702.1	$(9^{+}) \to 8^{(+)}$	10.0(2.7)	0.86(0.19)
1326.5	4244.1	2917.3	$(13^{+}) \to (11^{+})$	< 2.0	
1408.2	3165.9	1757.3	$12^{(+)} \to 10^{(+)}$	42.9(4.7)	1.44(0.20)
1491.5	3967.9	2476.5	$(13^{+}) \to 11^{(+)}$	4.1(2.5)	
1657.8	4823.6	3165.9	$14^{(+)} \to 12^{(+)}$	6.8(4.8)	

bands in ^{84}Rb may be considered as candidate chiral doublet bands.

To gain a better understanding of the positive-parity doublet bands in ^{84}Rb, we have carried out calculations based on the triaxial particle rotor model (TPRM) [33–37]. In the TPRM calculations, several parameters are involved. The quadrupole deformation $\beta_2 = 0.28$ was obtained from the triaxial relativistic mean-field (RMF) [38–42] calculations for the $\pi g_{9/2} \otimes \nu g_{9/2}$ configuration in ^{84}Rb. Accordingly, the single-j shell Hamiltonian parameter is defined as 0.551 MeV [37]. To preserve the number of particles, the proton and neutron Fermi surfaces of ^{84}Rb are placed in the $\pi g_{9/2}[431]3/2$ and $\nu g_{9/2}[404]9/2$ orbitals, respectively. The moment of inertia was adjusted to reproduce the trend of the energy spectra and the calculation of the electromagnetic transition probabilities followed the process described in Refs. [33–36]. Because of the γ softness in ^{84}Rb [19–21,43], the γ deformation was adjusted to achieve a good description of the experiment data; the approach has been successfully applied to study the level structures in ^{84}Rb [19,20]. It is found that the calculated results with $\gamma = 27^{\circ}$ was the optimal agreement with the experimental data.

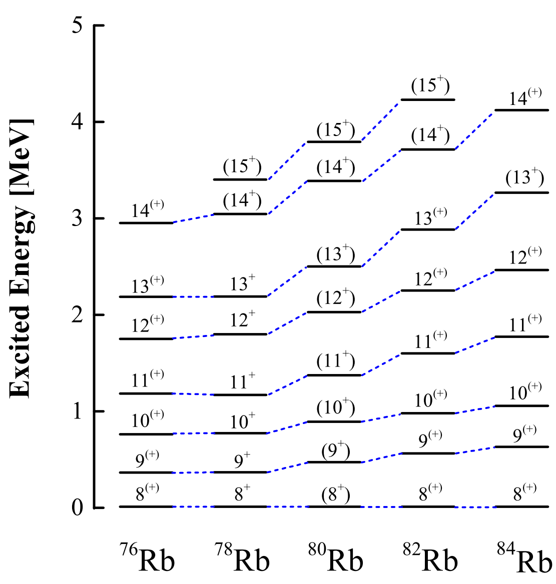

FIG. 4. The systematics of the positive-parity yrast states in ^{76}Rb [24], ^{78}Rb [25], ^{80}Rb [26], ^{82}Rb [20], and ^{84}Rb in this work.

The calculated $E(I)$, $S(I)$, and $B(M1)/B(E2)$ ratios for the doublet bands in ^{84}Rb are presented in Fig. 5, together with the corresponding experimental data. As shown in Fig. 5, the TPRM calculations are in reasonable agreement with the experimental data, which supports the present configuration assignment and allows us to further investigate the chiral geometry for the doublet bands in ^{84}Rb.

To investigate the chiral geometry in ^{84}Rb, the root-mean-square values of the angular momentum components for the core $R_k = \sqrt{\langle \hat{R}_k^2 \rangle}$, the valence proton $J_{pk} = \sqrt{\langle \hat{j}_{pk}^2 \rangle}$, and the valence neutron $J_{nk} = \sqrt{\langle \hat{j}_{nk}^2 \rangle}$ $(k = i, l, s)$ of the doublet

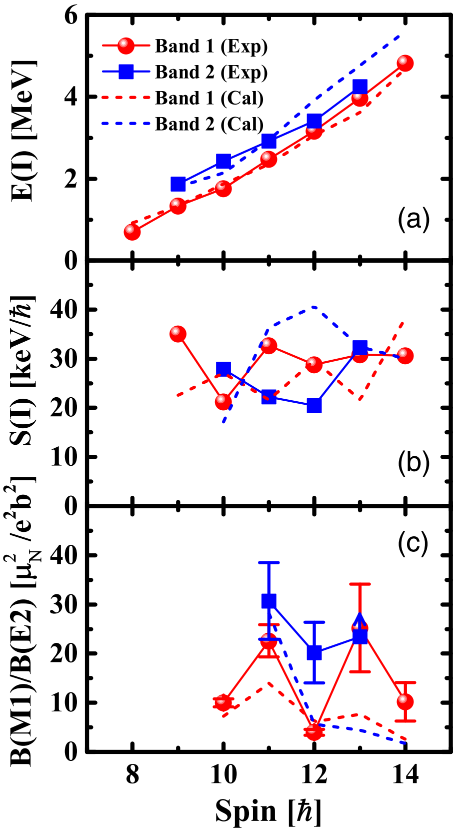

FIG. 5. Experimental excitation energies, energy staggering parameter $S(I) = [E(I) - E(I-1)]/2I$, and $B(M1)/B(E2)$ ratios for the positive-parity doublet bands in ^{84}Rb as a function of spin in comparison with the TPRM calculations.

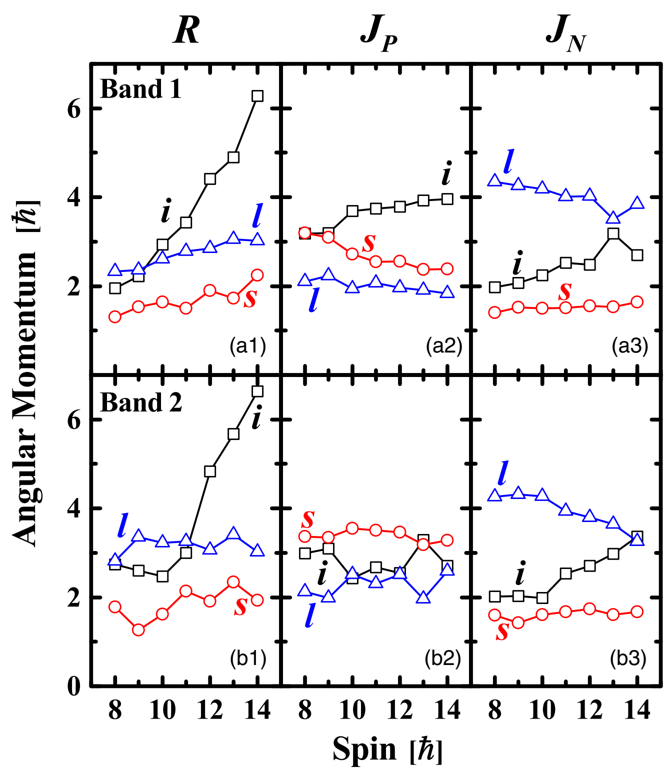

FIG. 6. The root-mean-square components along the intermediate (i, squares), short (s, circles), and long (l, triangles) axes of the core, valence proton, and valence neutron angular momenta calculated as functions of spin I by means of the TPRM for the positive-parity doublet bands in ^{84}Rb.

bands are calculated and presented in Fig. 6. As shown in Fig. 6, the angular momentum of the core and $\boldsymbol{J}_n$ mainly lie along the intermediate and long axes, respectively. Meanwhile, $\boldsymbol{J}_p$ for band 1 mainly aligns along the intermediate axis, and the orientations of $\boldsymbol{J}_p$ for band 2 show a large mixture between the short and intermediate axes. The present coupling pattern departs from the static chirality [44], which indicates the characteristics of chiral vibrations for candidate chiral doublet bands in ^{84}Rb. The lack of static chirality may be caused by the Fermi surface of the proton in ^{84}Rb placed in the $\pi g_{9/2}[431]3/2$ orbital instead of the $\pi g_{9/2}[440]1/2$ orbital.

From the above discussion, the positive-parity doublet bands in ^{84}Rb are proposed to be candidate chiral vibrational bands, which makes ^{84}Rb the first $Z = 37$ chiral nucleus in the $A \approx 80$ mass region. The present work extends the border of the chiral island in the $A \approx 80$ mass region to $Z = 37$, which allows us to investigate the evolution of chiral geometry with the proton number increasing. Figure 7 presents the excitation energies $E(I)$, the energy differences $\triangle E(I)$, the energy staggering parameter $S(I)$, and the kinematic moments of inertia $J^{(1)}$ for chiral doublet bands with $\pi g_{9/2} \otimes \nu g_{9/2}$ configuration in ^{78}Br [12], ^{80}Br [11], ^{82}Br [13], and ^{84}Rb as a function of spin. As shown in Fig. 7, ^{84}Rb shows some differences in comparison with ^{78}Br, ^{80}Br, and ^{82}Br. The energy differences in ^{84}Rb show a sharp decreasing at $I = 10\hbar$ rather than nearly constant values in ^{78,80,82}Br. In addition, comparing with the close $S(I)$ values and the kinematic moments of inertia for the doublet bands in ^{78,80,82}Br, these values in ^{84}Rb show some differences for the doublet bands. Similar experimental properties have been found in candidate chiral doublet bands of ^{106}Ag, and were suggested to be caused by the chiral vibrations resulting from a large degree of γ softness [45]. Therefore, the doublet bands in ^{84}Rb might be interpreted similarly, i.e., the chiral vibrational bands occur because of the γ softness. Remarkably, the interpretation of the doublet bands in ^{106}Ag is still an open question prompting many discussions [46–48]. Further measurements on lifetime and g factor for the doublet bands in ^{84}Rb are highly expected to obtain an unambiguous conclusion.

IV. CONCLUSION

In summary, high-spin states in ^{84}Rb have been studied using the ^{76}Ge(^{11}B, $3n$) reaction at a beam energy of 36 MeV. The positive-parity doublet bands in ^{84}Rb have been extended. The experimental properties and the theoretical calculations suggest that the doublet bands in ^{84}Rb are candidate chiral doublet bands with the $\pi g_{9/2} \otimes \nu g_{9/2}$ configuration. The present work extends the border of the chiral island in the $A \approx 80$ mass region to $Z = 37$. The calculated root-mean-square values of the angular momentum components of the doublet bands in ^{84}Rb and the systematic comparison of the

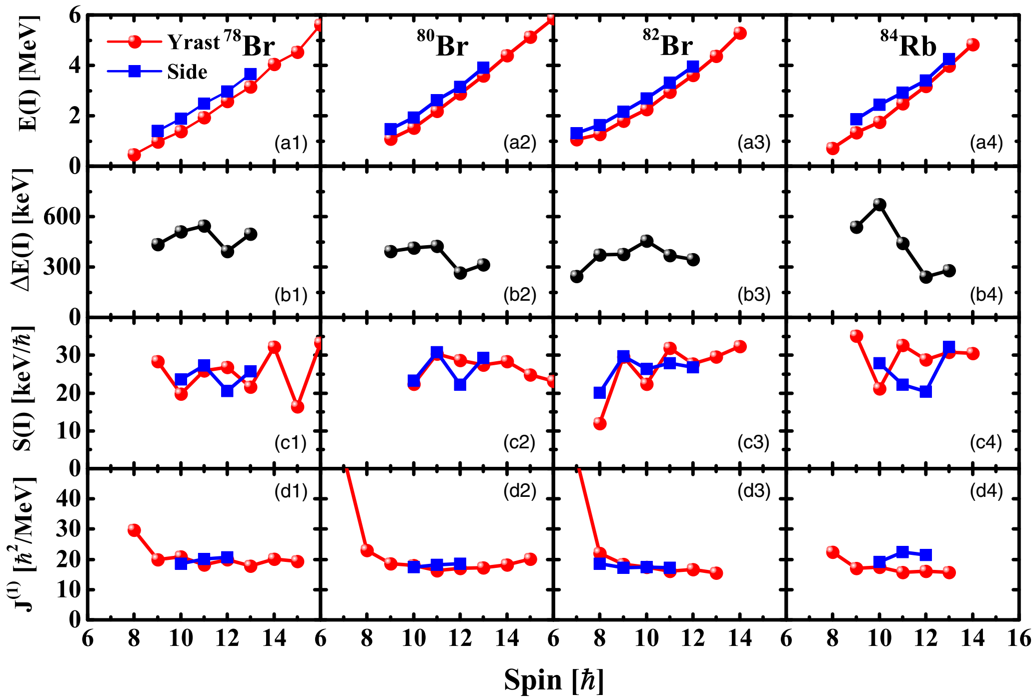

FIG. 7. The excitation energies $E(I)$ (a), the energy differences $\triangle E(I)$ (b), the energy staggering parameter $S(I)$ (c), and the kinematic moments of inertia $J^{(1)}$ (d) as a function of spin for the candidate chiral doublet bands with the $\pi g_{9/2} \otimes \nu g_{9/2}$ configuration in ^{78}Br [12], ^{80}Br [11], ^{82}Br [13], and ^{84}Rb (present work).

candidate chiral bands in the $A \approx 80$ mass region suggest the doublet bands in ^{84}Rb as chiral vibration resulting from the γ softness.

ACKNOWLEDGMENTS

This work is partly supported by the Shandong Natural Science Foundation of Shandong Province (No. JQ201701, No. ZR2020ZD30), the National Natural Science Foundation of China (No. 11622540, No. 11705102), and the Young Scholars Program of Shandong University, Weihai. The numerical calculations in this paper were done on the supercomputing system in the Supercomputing Center in Shandong University, Weihai. The authors thank the staff of the China Institute of Atomic Energy (CIAE) for their technical support during this experiment.

[1] S. Frauendorf and J. Meng, Nucl. Phys. A **617**, 131 (1997).
[2] S. Frauendorf, Rev. Mod. Phys. **73**, 463 (2001).
[3] J. Meng, B. Qi, S. Q. Zhang, and S. Y. Wang, Mod. Phys. Lett. A **23**, 2560 (2008).
[4] J. Meng and S. Q. Zhang, J. Phys. G **37**, 064025 (2010).
[5] R. A. Bark, E. O. Lieder, R. M. Lieder, E. A. Lawrie, J. J. Lawrie, S. P. Bvumbi, N. Y. Kheswa, S. S. Ntshangase, T. E. Madiba, P. L. Masiteng, S. M. Mullins, S. Murray, P. Papka, and O. Shirinda, Int. J. Mod. Phys. E **23**, 1461001 (2014).
[6] J. Meng and P. W. Zhao, Phys. Scr. **91**, 053008 (2016).
[7] A. A. Raduta, Prog. Part. Nucl. Phys. **90**, 241 (2016).
[8] K. Starosta and T. Koike, Phys. Scr. **92**, 093002 (2017).
[9] B. W. Xiong and Y. Y. Wang, At. Data Nucl. Data Tables **125**, 193 (2019).
[10] S. Y. Wang, Chin. Phys. C **44**, 112001 (2020).
[11] S. Y. Wang, B. Qi, L. Liu, S. Q. Zhang, H. Hua, X. Q. Li, Y. Y. Chen, L. H. Zhu, J. Meng, S. M. Wyngaardt, P. Papka, T. T. Ibrahim, R. A. Bark, P. Datta, E. A. Lawrie, J. J. Lawrie, S. N. T. Majola, P. L. Masiteng, S. M. Mullins, J. Gál *et al.*, Phys. Lett. B **703**, 40 (2011).
[12] C. Liu, S. Y. Wang, R. A. Bark, S. Q. Zhang, J. Meng, B. Qi, P. Jones, S. M. Wyngaardt, J. Zhao, C. Xu, S.-G. Zhou, S. Wang, D. P. Sun, L. Liu, Z. Q. Li, N. B. Zhang, H. Jia, X. Q. Li, H. Hua, Q. B. Chen *et al.*, Phys. Rev. Lett. **116**, 112501 (2016).
[13] C. Liu, S. Y. Wang, B. Qi, S. Wang, D. P. Sun, Z. Q. Li, R. A. Bark, P. Jones, J. J. Lawrie, L. Masebi, M. Wiedeking, J. Meng, S. Q. Zhang, H. Hua, X. Q. Li, C. G. Li, R. Han, S. M. Wyngaardt, B. H. Sun, L. H. Zhu, T. D. Bucher, B. V. Kheswa, K. L. Malatji, J. Ndayishimye, O. Shirinda, T. Dinoko, N. Khumalo, E. A. Lawrie, and S. S. Ntshangase, Phys. Rev. C **100**, 054309 (2019).
[14] H. Y. Wu, Z. H. Li, H. Tan, H. Hua, J. Li, W. Henning, W. K. Warburton, D. W. Luo, X. Wang, X. Q. Li, S. Q. Zhang, C. Xu, Z. Q. Chen, C. G. Wu, Y. Jin, J. Lin, D. X. Jiang, and Y. L. Ye, Nucl. Instrum. Methods Phys. Res. A **975**, 164200 (2020).
[15] H. Tan, W. Henning, M. Walby, A. F. Labruyere, J. Harris, D. Breus, P. Grudberg, W. K. Warburton, C. Vaman, T. Glasmacher, P. Mantica, D. Miller, K. Starosta, and P. Voss,

in *Nuclear Science Symposium Conference Record* (IEEE, Washington, DC, 2008), p. 3196.
[16] M. Piiparinen, A. Ataç, J. Blomqvist, G. B. Hagemann, B. Herskind, R. Julin, S. Juutinen, A. Lampinen, J. Nyberg, G. Sletten, P. Tikkanen, S. Törmänen, A. Virtanen, and R. Wyss, Nucl. Phys. A **605**, 191 (1996).
[17] R. Schwengner, G. Rainovski, H. Schnare, A. Wagner, S. Frauendorf, F. Dönau, A. Jungclaus, M. Hausmann, O. Yordanov, K. P. Lieb, D. R. Napoli, G. deAngelis, M. Axiotis, N. Marginean, F. Brandolini, and C. Rossi Alvarez, Phys. Rev. C **80**, 044305 (2009).
[18] G. B. Han, S. X. Wen, X. G. Wu, X. A. Liu, G. S. Li, G. J. Yuan, Z. H. Peng, P. K. Weng, C. X. Chun, Y. J. Ma, and J. B. Lu, Chin. Phys. Lett. **16**, 487 (1999).
[19] H. Schnare, R. Schwengner, S. Frauendorf, F. Dönau, L. Kaübler, H. Prade, A. Jungclaus, K. P. Lieb, C. Lingk, S. Skoda, J. Eberth, G. deAngelis, A. Gadea, E. Farnea, D. R. Napoli, C. A. Ur, and G. Lo Bianco, Phys. Rev. Lett. **82**, 4408 (1999).
[20] R. Schwengner, G. Rainovski, H. Schnare, A. Wagner, F. Dönau, A. Jungclaus, M. Hausmann, O. Iordanov, K. P. Lieb, D. R. Napoli, G. de Angelis, M. Axiotis, N. Marginean, F. Brandolini, and C. Rossi Alvarez, Phys. Rev. C **66**, 024310 (2002).
[21] S. F. Shen, G. B. Han, S. X. Wen, F. Pan, J. Y. Zhu, J. Z. Gu, J. P. Draayer, X. G. Wu, L. H. Zhu, C. Y. He, G. S. Li, B. B. Yu, T. D. Wen, and Y. P. Yan, Phys. Rev. C **82**, 014306 (2010).
[22] A. Grütter, Int. J. Appl. Radiat. Isot. **33**, 456 (1982).
[23] J. Döring, G. Winter, L. Funke, L. Käubler, and W. Wagner, Z. Phys. A **338**, 457 (1991).
[24] R. Wadsworth, I. Ragnarsson, B. G. Carlsson, H. L. Ma, P. J. Davies, C. Andreoiu, R. A. E. Austin, M. P. Carpenter, D. Dashdorj, S. J. Freeman, P. E. Garrett, J. Greene, A. Görgen, D. G. Jenkins, F. J. Theasby, P. Joshi, A. O. Macchiavelli, F. Moore, G. Mukherjee, W. Reviol, D. G. Sarantites, C. E. Svensson, and J. J. Valiente-Dobón, Phys. Lett. B **701**, 306 (2011).
[25] R. A. Kaye, J. Döring, J. W. Holcomb, G. D. Johns, T. D. Johnson, M. A. Riley, G. N. Sylvan, P. C. Womble, V. A. Wood, S. L. Tabor, and J. X. Saladin, Phys. Rev. C **54**, 1038 (1996).
[26] M. A. Cardona, G. García Bermúdez, R. A. Kaye, G. Z. Solomon, and S. L. Tabor, Phys. Rev. C **61**, 044316 (2000).
[27] K. Starosta, T. Koike, C. J. Chiara, D. B. Fossan, D. R. LaFosse, A. A. Hecht, C. W. Beausang, M. A. Caprio, J. R. Cooper, R. Krücken, J. R. Novak, N. V. Zamfir, K. E. Zyromski, D. J. Hartley, D. Balabanski, J.-y. Zhang, S. Frauendorf, and V. I. Dimitrov, Phys. Rev. Lett. **86**, 971 (2001).
[28] T. Koike, K. Starosta, C. J. Chiara, D. B. Fossan, and D. R. LaFosse, Phys. Rev. C **63**, 061304(R) (2001).
[29] G. Rainovski, E. S. Paul, H. J. Chantler, P. J. Nolan, D. G. Jenkins, R. Wadsworth, P. Raddon, A. Simons, D. B. Fossan, T. Koike, K. Starosta, C. Vaman, E. Farnea, A. Gadea, T. Kröll, R. Isocrate, G. de Angelis, D. Curien, and V. I. Dimitrov, Phys. Rev. C **68**, 024318 (2003).
[30] T. Koike, K. Starosta, C. Vaman, T. Ahn, D. B. Fossan, R. M. Clark, M. Cromaz, I. Y. Lee, and A. O. Macchiavelli, in *Frontiers of Nuclear Structure, FNS2002, Berkeley, CA, 2002*, edited by P. Fallon and R. Clark, AIP Conf. Proc. No. 656 (AIP New York, 2003), p. 160.
[31] T. Koike, K. Starosta, and I. Hamamoto, Phys. Rev. Lett. **93**, 172502 (2004).
[32] S. Y. Wang, S. Q. Zhang, B. Qi, and J. Meng, Chin. Phys. Lett. **24**, 664 (2007).
[33] S. Y. Wang, S. Q. Zhang, B. Qi, and J. Meng, Phys. Rev. C **75**, 024309 (2007).
[34] S. Q. Zhang, B. Qi, S. Y. Wang, and J. Meng, Phys. Rev. C **75**, 044307 (2007).
[35] S. Y. Wang, S. Q. Zhang, B. Qi, J. Peng, J. M. Yao, and J. Meng, Phys. Rev. C **77**, 034314 (2008).
[36] S. Y. Wang, B. Qi, and D. P. Sun, Phys. Rev. C **82**, 027303 (2010).
[37] S. Y. Wang, B. Qi, and S. Q. Zhang, Chin. Phys. Lett. **26**, 052102 (2009).
[38] J. Meng, J. Peng, S. Q. Zhang, and S.-G. Zhou, Phys. Rev. C **73**, 037303 (2006).
[39] J. Peng, H. Sagawa, S. Q. Zhang, J. M. Yao, Y. Zhang, and J. Meng, Phys. Rev. C **77**, 024309 (2008).
[40] J. M. Yao, B. Qi, S. Q. Zhang, J. Peng, S. Y. Wang, and J. Meng, Phys. Rev. C **79**, 067302 (2009).
[41] J. Li, S. Q. Zhang, and J. Meng, Phys. Rev. C **83**, 037301 (2011).
[42] B. Qi, H. Jia, C. Liu, and S. Y. Wang, Phys. Rev. C **98**, 014305 (2018).
[43] W. Nazarewicz, in *High Spin Physics and Gamma-soft Nuclei* edited by J. X. Saladin, R. A. Sorensen, and C. M. Vincent (World Scientific, Singapore, 1991), p. 406.
[44] C. Vaman, S. Lakshmi, and P. K. Joshi, Phys. Lett. B **92**, 032501 (2004).
[45] P. Joshi, M. P. Carpenter, D. B. Fossan, T. Koike, E. S. Paul, G. Rainovski, K. Starosta, C. Vaman, and R. Wadsworth, Phys. Rev. Lett. **98**, 102501 (2007).
[46] E. O. Lieder, R. M. Lieder, R. A. Bark, Q. B. Chen, S. Q. Zhang, J. Meng, E. A. Lawrie, J. J. Lawrie, S. P. Bvumbi, N. Y. Kheswa, S. S. Ntshangase, T. E. Madiba, P. L. Masiteng, S. M. Mullins, S. Murray, P. Papka, D. G. Roux, O. Shirinda, Z. H. Zhang, P. W. Zhao, Z. P. Li, J. Peng, B. Qi, S. Y. Wang, Z. G. Xiao, and C. Xu, Phys. Rev. Lett. **112**, 202502 (2014).
[47] N. Rather, P. Datta, S. Chattopadhyay, S. Rajbanshi, A. Goswami, G. H. Bhat, J. A. Sheikh, S. Roy, R. Palit, S. Pal, S. Saha, J. Sethi, S. Biswas, P. Singh, and H. C. Jain, Phys. Rev. Lett. **112**, 202503 (2014).
[48] P. W. Zhao, Y. K. Wang, and Q. B. Chen, Phys. Rev. C **99**, 054319 (2019).